Internal/External Offsets in the FOS Wavelength Calibration

G. A. Kriss, W. P. Blair, and A. F. Davidsen
The Johns Hopkins University

Instrument Science Report CAL/FOS-070
February 1992

Abstract

In September 1991 the M1.6Ve star AU Microscopii was observed with gratings G130H, G190H, and G160L on the blue side, and gratings G190H, G270H, G400H, and G570H on the red side to evaluate offsets in the FOS wavelength calibration between the internal Pt-Cr-Ne calibration lamps and an external source of light. Observations of the internal lamps were obtained with the identical gratings either before or after the observation of AU Mic without changing the position of the filter/grating wheel. After correction for the geomagnetically induced motion problem on the red side, we find a mean offset ($X_{internal} - X_{external}$) of +0.176 diodes with a dispersion of 0.105 diodes. On the blue side, the offset ($X_{internal} - X_{external}$) is −0.102 diodes with a dispersion of 0.100 diodes. Allowing for the scatter in the in-flight measurements, the offsets are similar in size and character to those observed in pre-flight tests. Given the observed dispersion of ~0.1 diode in our measured offsets, velocity measurements based on single lines in FOS spectra have a limiting accuracy of roughly 20 km s^{-1}.

1 Introduction

Systematic offsets between wavelengths derived from the internal calibration lamps and external sources have always been noticed for the FOS (Sirk and Bohlin 1987; Bohlin, Sirk, and Hartig 1987; Blair, Kriss, and Davidsen 1988). The optics associated with the internal lamps do not fully illuminate the spectrograph entrance beam, and chromatic aberration in the comparison lamp lens causes the illumination to vary with wavelength. Pre-flight checks on the internal/external offsets used a Pt-Cr-Ne lamp in the Space Telescope Optical Simulator (STOS) to provide the external illumination of the FOS entrance port. This uniformly illuminates the spectrograph optics, but it does not truly simulate the illumination provided by a point source as imaged by the optical telescope assembly (OTA) of HST. Here we report on in-flight observations of a stellar source that give the first measure of the offsets an observer is likely to encounter in a typical observation with the FOS.

The star AU Microscopii (HD197481; GSSS 7457-641) is a dMe star (M1.6Ve) of the BY Draconis class. The visible light continuum is typical of late-type stars. In addition, AU Mic has strong Balmer series emission, emission from Ca II H and K, and strong UV line emission typical of the chromosphere and transition regions of late-type stars. The radial velocity is low ($cz_{\odot} = -2.1 \pm 1.0$ km s^{-1}) and there are no velocity shifts between the emission and absorption lines (Bopp and Fekel 1977). Observations of the UV lines with the

International Ultraviolet Explorer (IUE) show the lines to be narrow, even at high dispersion, with no velocity shifts between the various lines (Linsky *et al.* 1982; Ayres *et al.* 1983). It is thus an ideal target for investigating internal/external wavelength offsets in the FOS.

2 The Observations

We observed AU Mic on 10-11 September 1991 as part of Science Verification (SV) proposal 3316, which was designed to measure the internal/external wavelength offsets as well as determine line shapes through various FOS apertures to assess the impact of the degraded performance of the OTA on the line profiles for a point source. The line profile measurements will be discussed in another report. An earlier version of this proposal (SV 1317) failed because the proper motion of the star was not properly taken into account in specifying the coordinates.

To ensure the target was centered in the aperture for each set of observations, a peak-up target acquisition was used in successively smaller apertures. The final peak-up on each side was a 5×5 grid on 0.05" centers using the 0.3" circular aperture (the aperture used for the internal/external offset measurements). On the red side the final peak was in the center of the last scan pattern, but on the blue side, the peak was in one corner. This was the expected location, however, based on the results of the preceding coarser scan, and, judging from the relative counts at each position, we believe the target was centered to better than 0.03". The individual observations and the root filenames for the resulting data sets from both the blue and red side observation sequences are summarized in Table 1. All observations produced usable spectra, although the blue side observations of AU Mic were somewhat underexposed.

3 Data Reduction and Analysis

For our analysis we use the count-rate files *.C4H,*.C4D produced by the RSDP system. These data have been corrected for quarter-stepping and dead diodes and converted to count rates. Red-side data were corrected for the geomagnetically-induced motion problem (GIMP) by calculating the required correction factor with the IDL tool *fos_gimp_corr* (Junkarrinen 1990) and shifting the FOS spectra appropriately using the *imshift* task in the *images* package of IRAF. Linear interpolation of pixels was used in doing the shifts. The GIMP correction moves the spectra back to the position on the diode array corresponding to zero magnetic field threading the detectors.

New dispersion solutions for each detector/grating combination were obtained using Don Lindler's IRAF/STSDAS implementation of the Sirk and Bohlin algorithms described in CAL/FOS-026. Line lists prepared as part of the FOS in-flight wavelength calibration (Kriss, Blair, and Davidsen 1990) were identified in the calibration spectra and centroided by the task *linefind* in the FOS package of STSDAS using the cross-correlation algorithm described in CAL/FOS-026. We used the same peak-finding kernel for the cross-correlation, a three-point triangle with relative weights 0.8, 1.0, 0.8, as used by Sirk and Bohlin.

Using the task *dispfity*, also in the FOS package of STSDAS, the diffraction grating spectra were fit with a cubic polynomial with uniform weighting for each line in the fit. The resulting dispersion solutions have root-mean-square residuals typically less than 0.05 diodes. Compared to template spectra obtained during orbital verification, the mean dispersions are similar, but the zero points differ by several tenths of a diode in some cases. These zero-point shifts are probably due to filter/grating wheel non-repeatability.

We generated new wavelength files based on the new dispersion solutions. Linearized versions of the FOS spectra suitable for measurements using the *splot* task in the *onedspec* package of IRAF were then produced using the *resample* task in the FOS package. We used "sinc" interpolation with the default 35 pixel Hanning window in calculating the linearized spectra. The most prominent emission and absorption lines in each spectrum were identified. The G190H and G270H spectra are dominated by emission from many multiplets of Fe II. Only those multiplets which were definitely resolved or easily deblended into two components were used in the internal/external offset analysis. Many blends whose positions were not used in the analysis were used to verify the correct identification of the Fe II lines. Positions were measured by fitting Gaussian profiles to the lines using the 'd' function in *splot*. This aided in deblending several strong, closely spaced emission and absorption lines. The great majority of the measured lines had only ~200 total counts, with some lines having as few as 100 total counts. Centroids could be determined with an accuracy of only ~0.06 diodes in typical cases, and errors for the weaker lines could approach 0.15 diodes.

Historically, offsets between the internal calibration lamps in the FOS and an external lamp have always been expressed in terms of the observed difference in the X detector coordinate in the sense $\Delta X_{I/E} = X_{internal} - X_{external}$. Since the identical emission lines were observed in the internal and external spectra, $\Delta x_{I/E}$ was easily obtained simply by making all measurements in diode space without an intermediate wavelength scale. The situation presented by the AU Mic observations is more complex since one set of lines emitted by the internal lamps is used to determine a wavelength scale, and then the wavelengths of a different set of lines in an external source are measured on this wavelength scale. For consistency with previous analyses, it is helpful to transform the observations into detector coordinates. Since the non-linear terms in the dispersion relations for the gratings are small and do not affect the arithmetic signs of the following discussion, we assume the wavelength scale can be written as $\lambda = \lambda_0 + \Delta\lambda X$, where $\Delta\lambda$ is the mean dispersion of the spectrum. The detector X coordinate of a feature measured in the spectrum of an external object is then

$$X_{external} = \frac{(\lambda_{measured} - \lambda_0)}{\Delta\lambda} . \qquad (1)$$

If this spectral feature had actually been part of the spectrum generated by an internal lamp, it would have been centered on a detector coordinate given by

$$X_{internal} = \frac{(\lambda_{actual} - \lambda_0)}{\Delta\lambda} , \qquad (2)$$

where λ_{actual} is the wavelength of the feature as it enters the aperture of the telescope. This "actual" wavelength is the vacuum wavelength Doppler-shifted by the *observed* stellar radial velocity (+6 km s^{-1} for these observations). The *heliocentric* stellar radial velocity of –2.1 km s^{-1} is converted to an *observed* velocity by correcting for the earth's motion in the solar system using the *rvcorrect* task in the *astutil* package of IRAF. Motion of the spacecraft around the earth was not corrected; based on the times of observation relative to source occultations, however, we estimate that corrections for spacecraft motion are less than 5 km s^{-1}.

Internal/external offsets following the same convention used in previous CAL/FOS reports are thus given by

$$\Delta X_{I/E} = X_{internal} - X_{external} = (\lambda_{actual} - \lambda_{measured})/\Delta\lambda \qquad (3)$$

In Table 2 we list the measured wavelengths of emission and absorption lines from the AU Mic spectra and provide the vacuum wavelength for each line. In column 4 we give the offsets in wavelength as $\lambda_{actual} - \lambda_{measured}$. The offsets in wavelength are transformed to offsets in diodes in column 5 using equation (3).

The observed offsets ($X_{internal} - X_{external}$) are plotted against wavelength for each grating in Figure 1. These figures may be directly compared to the offsets shown by Blair *et al.* (1988). The character of the observed offsets is similar to pre-flight measurements of internal/external offsets in the FOS wavelength scale. The offsets are of the same order of magnitude, 0.1 to 0.2 diodes, but the mean values are different, and the striking variation with wavelength found by Blair *et al.* (1988) is not as pronounced. Grating G190H on the red side shows a mean offset of ~0.35 diodes on the red end that rapidly decreases to a mean of ~0.1 on the blue end. This may be compared to the same grating in Figure 6a of Blair *et al.* (1988) where the offset shows a slow monotonic decrease from +0.1 diodes on the red end to -0.15 diodes on the blue end — roughly the same change with wavelength, but a different overall mean. The AU Mic data for gratings G270H and G400H show little variation in wavelength. Much of the variation, however, could be masked by the relatively larger measurement errors in the AU Mic observations since the offsets in Blair *et al.* (1988) for these two gratings change by only ~0.2 diodes over the full range in wavelength. It is also possible that the illumination provided by a true point source imaged by the OTA is sufficiently different from that provided by the STOS (which presumably has no spherical aberration) that the variation of offsets with wavelength is different. Table 3 provides a summary of the offsets observed with each grating. The mean offset is given in column 3, the dispersion about the mean in column 4, and the number of spectral features used in calculating the mean and dispersion in the last column.

4 Updating the CDBS

As of mid-November 1991, the GIMP corrections on both the blue and the red sides have been implemented in the RSDP processing of the FOS spectra. The previous coefficients in the wavelength table CYCCS6 were obtained using spectra uncorrected for the GIMP. We have calculated the GIMP correction for the FOS template spectra used to obtain the coefficients in the database. Correcting the wavelength coefficients in CYCCS6 for offsets due to GIMP and the internal/external offsets are essentially identical problems. We discuss here the method used to calculate the corrections and describe the strategy followed to implement the corrections.

A GIMP correction ΔX_G shifts the spectrum such that $X_{cor} = X + \Delta X_G$. To update the coefficients for this shift we must find a transformation that leaves the wavelengths of the lines used for the wavelength calibration invariant under the coordinate change. For the gratings we thus have

$$c_0 + c_1 X + c_2 X^2 + c_3 X^3 = c_0' + c_1' X_{cor} + c_2' X_{cor}^2 + c_3' X_{cor}^3 . \qquad (4)$$

Substituting $X_{cor} = X + \Delta X_G$ into the right-hand side, expanding the polynomials, and then grouping like terms in X leads to the solution

$$c_0 = c_0' + c_1' \Delta X_G + c_2' \Delta X_G^2 + c_3' \Delta X_G^3 , \qquad (5.0)$$

$$c_1 = c_1' + 2c_2' \Delta X_G + 3c_3' \Delta X_G^2 , \qquad (5.1)$$

$$c_2 = c_2' + 3c_3'\Delta X_G \,, \tag{5.2}$$

$$c_3 = c_3' \,. \tag{5.3}$$

We then solve for the new coefficients to obtain

$$c_0' = c_0 - c_1\Delta X_G + c_2\Delta X_G^2 - c_3\Delta X_G^3 \,, \tag{6.0}$$

$$c_1' = c_1 - 2c_2\Delta X_G + 3c_3\Delta X_G^2 \,, \tag{6.1}$$

$$c_2' = c_2 - 3c_3\Delta X_G \,, \tag{6.2}$$

$$c_3' = c_3 \,. \tag{6.3}$$

The dispersion relation for the prisms is easier to update. For

$$\lambda = A_0 + \frac{A_1}{(X-X_0)} + \frac{A_1}{(X-X_0)^2} + \frac{A_1}{(X-X_0)^2} + \frac{A_1}{(X-X_0)^2} \,, \tag{7}$$

a GIMP correction ΔX_G is implemented simply by substituting $X_0' = X_0 + \Delta X_G$.

Corrections for an internal/external offset are analogous, but the conventions used in defining the offset have the opposite sign of the GIMP corrections. An internal/external offset $\Delta X_{I/E}$ defined by the convention "internal − external" implies $X_{cor} = X_{external} = X_{internal} - \Delta X_{I/E}$, hence

$$c_0' = c_0 + c_1\Delta X_{I/E} + c_2\Delta X_{I/E}^2 + c_3\Delta X_{I/E}^3 \,, \tag{8.0}$$

$$c_1' = c_1 + 2c_2\Delta X_{I/E} + 3c_3\Delta X_{I/E}^2 \,, \tag{8.1}$$

$$c_2' = c_2 + 3c_3\Delta X_{I/E} \,, \tag{8.2}$$

$$c_3' = c_3 \text{ , and} \tag{8.3}$$

$$X_0' = X_0 - \Delta X_{I/E} \,. \tag{8.4}$$

To correct the coefficients in CYCCS6 for both GIMP and internal/external offsets, we define a total correction $\Delta X_{tot} \equiv \Delta X_{I/E} - \Delta X_G$ that has the same sign as the internal/external offset correction and solve for new coefficients as given above in equations 8.0 - 8.4 for internal/external offsets. These new coefficients were incorporated into CYCCS6 for submission to the CDBS using the following strategy:

[1] All coefficients were corrected for GIMP using the current best estimates for the GIMP correction on both the blue and the red sides,

$\Delta X_G = 0.74$ diodes $(\cos(17°)B_X - \sin(17°)B_Y)$ on the blue side, and

$\Delta X_G = 2.95$ diodes $(\cos(17°)B_X - \sin(17°)B_Y)$ on the red side.

[2] Internal/external offsets for the detector and grating combinations measured here used the mean offsets given in Table 3. The offsets were assumed to be independent of aperture.

[3] For detector and disperser combinations not measured in this study, internal/external offsets were determined using the mean for all gratings for the given detector.

[4] Only entries for polarimetry mode "C" were updated in CYCCS6.

This update should now provide the best estimate of the FOS wavelength solution for all GIMP-corrected FOS spectra. Errors in the wavelength scale of several tenths of a diode can

still be expected, however, due to filter/grating wheel non-repeatability. Observations requiring accurate wavelength scales should always include appropriate wavelength calibrations either directly before or after the observations, before the filter/grating wheel is moved.

5 Conclusions

Observations of the dwarf emission line star AU Mic have provided the first in-flight measurement of offsets in the wavelength scale between the internal calibration lamps and a known external point source. The offsets are similar in character and magnitude to those seen in pre-flight testing of the FOS. On the red side, the mean offset ($X_{internal} - X_{external}$) is +0.176 diodes with a dispersion of 0.105 diodes about that value. On the blue side, the mean offset ($X_{internal} - X_{external}$) is –0.102 with a dispersion of 0.100. Given the observed dispersion in our measured values, velocity measurements based on *single* lines in FOS spectra have a limiting accuracy of roughly 20 km s^{-1}, if simultaneous wavelength calibrations are made. Velocity errors will decrease for measurement of more lines. If simultaneous wavelength calibrations are not made, however, non-repeatability in the positioning of the filter/grating wheel will dominate errors in the wavelength scale.

References

Ayres, T. R., Eriksson, K., Linsky, J. L., and Stencel, R. E. 1983, ApJ, 270, L17.

Blair, W. P., Kriss, G. A., and Davidsen, A. F. 1988. CAL/FOS-056, *FOS Internal/External Offsets.*

Bohlin, R., Sirk, M., and Hartig, G. 1987. CAL/FOS-044, *Limiting Accuracy of FOS Wavelength Calibration.*

Bopp, B. W., and Fekel, Jr., F. 1977, AJ, 82, 490.

Junkarrinen, V., Beaver, E., Cohen, R., and Lyons, R. 1990. CAL/FOS-066, *Sensitivity of the FOS Red Digicon to External B-fields.*

Kriss, G. A., Blair, W. P., and Davidsen, A. F. 1988. CAL/FOS-054, *Revised FOS Wavelength Calibration.*

_____. 1991. CAL/FOS-067, *In-Flight FOS Wavelength Calibration — Template Spectra.*

Linsky, J. L., Bornmann, P. L., Carpenter, K. G., Wing, R. F., Giampapa, M. S., Warden, S. P., and Hege, E. K. 1982, ApJ, 260, 670.

Sirk, M., and Bohlin, R. 1986. CAL/FOS-026, *FOS Wavelength Calibration.*

_____. 1987. CAL/FOS-041, *Wavelength Offsets among Internal Lamps and External Sources.*

TABLE 1
Observations for Internal/External Offset Measurements

Filename	Target	DET	DISP	APER	DATE (UT)	TIME (UT)	EXP (s)
y0q70101t	AU MIC	BLUE	G400H	A-1/4.3	10SEP91	19:31	0.10
y0q70102t	AU MIC	BLUE	G400H	B-3/1.0	10SEP91	20:53	1.00
y0q70103t	AU MIC	BLUE	G400H	B-2/0.3	10SEP91	21:06	1.00
y0q70104t	AU MIC	BLUE	G400H	B-2/0.3	10SEP91	22:17	1.00
y0q70105t	AU MIC	BLUE	G190H	B-1/0.5	10SEP91	22:41	29.25
y0q70106t	AU MIC	BLUE	G130H	B-1/0.5	10SEP91	22:46	13.00
y0q70107t	AU MIC	BLUE	G150H	B-1/0.5	10SEP91	22:50	13.00
y0q70108t	AU MIC	BLUE	G190H	B-3/1.0	10SEP91	22:56	20.25
y0q70109t	AU MIC	BLUE	G130H	B-3/1.0	10SEP91	23:01	9.00
y0q7010at	AU MIC	BLUE	G150H	B-3/1.0	10SEP91	23:53	9.00
y0q7010bt	AU MIC	BLUE	G190H	A-1/4.3	11SEP91	00:00	11.25
y0q7010ct	AU MIC	BLUE	G130H	A-1/4.3	11SEP91	00:04	5.00
y0q7010dt	AU MIC	BLUE	G150H	A-1/4.3	11SEP91	00:08	5.00
y0q7010et	AU MIC	BLUE	G190H	B-2/0.3	11SEP91	00:17	40.00
y0q7010ft	WAVE	BLUE	G190H	B-2/0.3	11SEP91	00:20	6.00
y0q7010gt	WAVE	BLUE	G130H	B-2/0.3	11SEP91	00:25	15.00
y0q7010ht	AU MIC	BLUE	G130H	B-2/0.3	11SEP91	00:29	17.50
y0q7010it	AU MIC	BLUE	G150H	B-2/0.3	11SEP91	00:33	17.50
y0q7010jt	WAVE	BLUE	G150H	B-2/0.3	11SEP91	00:37	6.00
y0q7010kt	AU MIC	BLUE	CAM	C-2/0.25×2.0	11SEP91	01:36	0.25
y0q7010lt	AU MIC	BLUE	G190H	C-2/0.25×2.0	11SEP91	01:46	29.25
y0q7010mt	AU MIC	BLUE	G130H	C-2/0.25×2.0	11SEP91	01:51	13.00
y0q7010nt	AU MIC	BLUE	G150H	C-2/0.25×2.0	11SEP91	01:55	13.00
y0q70201t	AU MIC	RED	G780H	A-1/4.3	11SEP91	03:22	0.10
y0q70202t	AU MIC	RED	G780H	B-3/1.0	11SEP91	03:37	0.20
y0q70203t	AU MIC	RED	G780H	B-2/0.3	11SEP91	04:44	0.50
y0q70204t	AU MIC	RED	G780H	B-2/0.3	11SEP91	05:06	5.00
y0q70205t	AU MIC	RED	G270H	B-1/0.5	11SEP91	06:22	32.50
y0q70206t	AU MIC	RED	G190H	B-1/0.5	11SEP91	06:28	32.50
y0q70207t	AU MIC	RED	G570H	B-1/0.5	11SEP91	06:56	19.50
y0q70208t	AU MIC	RED	G400H	B-1/0.5	11SEP91	07:01	19.50
y0q70209t	AU MIC	RED	G270H	B-3/1.0	11SEP91	07:07	22.50
y0q7020at	AU MIC	RED	G190H	B-3/1.0	11SEP91	07:58	32.14
y0q7020bt	AU MIC	RED	G570H	B-3/1.0	11SEP91	08:18	13.50
y0q7020ct	AU MIC	RED	G400H	B-3/1.0	11SEP91	08:23	13.50
y0q7020dt	AU MIC	RED	G270H	A-1/4.3	11SEP91	08:29	12.50
y0q7020et	AU MIC	RED	G190H	A-1/4.3	11SEP91	08:35	31.25
y0q7020ft	AU MIC	RED	G570H	A-1/4.3	11SEP91	09:33	7.50
y0q7020gt	AU MIC	RED	G400H	A-1/4.3	11SEP91	09:37	7.50
y0q7020ht	AU MIC	RED	G270H	B-2/0.3	11SEP91	09:47	47.50
y0q7020it	WAVE	RED	G270H	B-2/0.3	11SEP91	09:50	2.50
y0q7020jt	WAVE	RED	G190H	B-2/0.3	11SEP91	11:10	6.00
y0q7020kt	AU MIC	RED	G190H	B-2/0.3	11SEP91	11:15	31.67
y0q7020lt	AU MIC	RED	G570H	B-2/0.3	11SEP91	12:48	26.25
y0q7020mt	WAVE	RED	G570H	B-2/0.3	11SEP91	12:51	1.50
y0q7020nt	WAVE	RED	G400H	B-2/0.3	11SEP91	12:55	1.00

TABLE 1 (cont.)
Observations for Internal/External Offset Measurements

Filename	Target	DET	DISP	APER	DATE (UT)	TIME (UT)	EXP (s)
y0q7020ot	AU MIC	RED	G400H	B-2/0.3	11SEP91	12:59	25.00
y0q7020pt	AU MIC	RED	G780H	C-2/0.25×2.0	11SEP91	13:10	0.50
y0q7020qt	AU MIC	RED	G270H	C-2/0.25×2.0	11SEP91	13:20	32.50
y0q7020rt	AU MIC	RED	G190H	C-2/0.25×2.0	11SEP91	14:26	32.50
y0q7020st	AU MIC	RED	G570H	C-2/0.25×2.0	11SEP91	14:54	19.50
y0q7020tt	AU MIC	RED	G400H	C-2/0.25×2.0	11SEP91	14:59	19.50

TABLE 2
Wavelength Offsets Measured in AU Mic Spectra

Line	λ_{vac} (Å)	$\lambda_{measured}$ (Å)	$\lambda_{actual} - \lambda_{measured}$ (Å)	$X_{internal} - X_{external}$ (diodes)	DET	DISP
Lyα	1215.668	1215.887	−0.195	−0.194	BLUE	G130H
C II	1335.708	1335.841	−0.106	−0.106	BLUE	G130H
C IV	1548.185	1548.515	−0.299	−0.297	BLUE	G130H
C IV	1550.774	1550.924	−0.119	−0.118	BLUE	G130H
C I	1561.121	1561.369	−0.217	−0.215	BLUE	G130H
He II	1640.458	1640.582	−0.091	−0.062	BLUE	G190H
C I	1657.196	1657.507	−0.278	−0.189	BLUE	G190H
Si II	1808.012	1808.136	−0.088	−0.060	BLUE	G190H
Si II	1816.928	1817.040	−0.076	−0.052	BLUE	G190H
Al III	1854.716	1854.594	0.159	0.108	BLUE	G190H
C I	1930.905	1931.210	−0.266	−0.181	BLUE	G190H
C I	1993.620	1993.808	−0.148	−0.101	BLUE	G190H
Fe II	2280.620	2280.733	−0.067	−0.046	BLUE	G190H
Lyα	1215.668	1215.609	0.083	0.012	BLUE	G160L
C II	1335.708	1335.817	−0.082	−0.012	BLUE	G160L
C IV	1549.048	1550.226	−1.147	−0.161	BLUE	G160L
C I	1561.121	1562.515	−1.363	−0.191	BLUE	G160L
He II	1640.458	1640.788	−0.297	−0.042	BLUE	G160L
C I	1657.196	1658.341	−1.112	−0.156	BLUE	G160L
Si II	1808.012	1807.234	0.814	0.114	BLUE	G160L
Si II	1816.928	1817.900	−0.936	−0.131	BLUE	G160L
Fe II	2382.762	2383.155	−0.345	−0.048	BLUE	G160L
Fe II	2479.196	2480.874	−1.628	−0.229	BLUE	G160L
He II	1640.458	1640.545	−0.054	0.038	RED	G190H
C I	1657.196	1657.501	−0.272	0.189	RED	G190H
Al II	1670.787	1670.939	−0.119	0.083	RED	G190H
Si II	1808.012	1808.093	−0.045	0.031	RED	G190H
Si II	1816.928	1817.178	−0.214	0.149	RED	G190H
Al III	1854.716	1854.883	−0.130	0.091	RED	G190H
Si III	1892.030	1892.126	−0.058	0.041	RED	G190H
C I	1930.905	1931.047	−0.103	0.072	RED	G190H
C I	1993.620	1993.784	−0.124	0.086	RED	G190H
Si I	2124.794	2124.830	0.007	−0.005	RED	G190H
Si I	2208.667	2208.985	−0.274	0.191	RED	G190H
Fe II	2249.878	2250.580	−0.657	0.458	RED	G190H
Fe II	2251.633	2252.316	−0.638	0.445	RED	G190H
Fe II	2253.815	2254.384	−0.524	0.365	RED	G190H
Fe II	2256.676	2257.109	−0.388	0.270	RED	G190H
Fe II	2280.620	2281.077	−0.411	0.287	RED	G190H
Fe II	2253.815	2254.114	−0.254	0.124	RED	G270H
Fe II	2280.620	2280.802	−0.136	0.067	RED	G270H
Fe II	2328.111	2328.576	−0.418	0.205	RED	G270H
Fe II	2338.724	2339.266	−0.495	0.242	RED	G270H
Fe II	2349.019	2349.435	−0.369	0.180	RED	G270H
Fe II	2359.840	2360.962	−1.075	0.525	RED	G270H

TABLE 2 (cont.)
Wavelength Offsets Measured in AU Mic Spectra

Line	λ_{vac} (Å)	$\lambda_{measured}$ (Å)	$\lambda_{actual} - \lambda_{measured}$ (Å)	$X_{internal} - X_{external}$ (diodes)	DET	DISP
Fe II	2374.460	2375.004	-0.496	0.243	RED	G270H
Fe II	2382.762	2383.235	-0.425	0.208	RED	G270H
Fe II	2389.356	2389.836	-0.432	0.211	RED	G270H
Fe II	2396.354	2396.645	-0.243	0.119	RED	G270H
Fe II	2399.972	2400.364	-0.344	0.168	RED	G270H
Fe II	2405.617	2406.026	-0.361	0.176	RED	G270H
Fe II	2414.044	2414.170	-0.078	0.038	RED	G270H
Fe II	2479.196	2479.708	-0.462	0.226	RED	G270H
Fe II	2494.014	2494.416	-0.352	0.172	RED	G270H
Fe II	2512.138	2512.475	-0.287	0.140	RED	G270H
Fe II	2563.775	2564.210	-0.384	0.188	RED	G270H
Fe II	2586.648	2587.126	-0.426	0.208	RED	G270H
Fe II	2599.681	2600.268	-0.535	0.261	RED	G270H
Fe II	2607.864	2608.209	-0.293	0.143	RED	G270H
Fe II	2612.653	2613.171	-0.466	0.228	RED	G270H
Fe II	2614.600	2615.069	-0.417	0.204	RED	G270H
Fe II	2618.397	2619.027	-0.578	0.282	RED	G270H
Fe II	2626.450	2626.929	-0.426	0.208	RED	G270H
Fe II	2629.076	2629.502	-0.373	0.183	RED	G270H
Fe II	2631.969	2632.367	-0.345	0.169	RED	G270H
Al II	2669.958	2670.224	-0.213	0.104	RED	G270H
Fe II	2740.357	2740.836	-0.424	0.207	RED	G270H
Fe II	2744.008	2744.397	-0.334	0.163	RED	G270H
Fe II	2756.549	2757.014	-0.410	0.200	RED	G270H
Fe II	2760.149	2760.524	-0.320	0.156	RED	G270H
Fe II	2769.752	2770.351	-0.544	0.266	RED	G270H
Fe II	2776.157	2776.651	-0.438	0.214	RED	G270H
Mg II	2796.347	2796.885	-0.482	0.236	RED	G270H
Mg II	2803.523	2804.021	-0.442	0.216	RED	G270H
Mg I	2852.965	2853.364	-0.342	0.167	RED	G270H
Fe II	2869.714	2870.082	-0.311	0.152	RED	G270H
Fe II	2881.602	2882.355	-0.695	0.340	RED	G270H
Fe II	2908.704	2909.105	-0.343	0.168	RED	G270H
Fe II	2917.656	2918.261	-0.547	0.267	RED	G270H
Fe II	2927.443	2927.960	-0.458	0.224	RED	G270H
Fe II	2940.364	2940.771	-0.348	0.170	RED	G270H
Fe II	2945.257	2945.867	-0.551	0.269	RED	G270H
Fe II	2954.636	2955.189	-0.494	0.241	RED	G270H
Fe II	2962.136	2962.872	-0.677	0.331	RED	G270H
Fe II	2971.384	2971.740	-0.297	0.145	RED	G270H
Fe II	2976.806	2977.143	-0.277	0.136	RED	G270H
Fe II	2986.413	2986.756	-0.283	0.138	RED	G270H
Fe II	3003.523	3004.036	-0.453	0.221	RED	G270H
Mn I	3229.024	3229.442	-0.353	0.173	RED	G270H
Mn I	3257.072	3257.492	-0.355	0.173	RED	G270H

TABLE 2 (cont.)
Wavelength Offsets Measured in AU Mic Spectra

Line	λ_{vac} (Å)	$\lambda_{measured}$ (Å)	$\lambda_{actual} - \lambda_{measured}$ (Å)	$X_{internal} - X_{external}$ (diodes)	DET	DISP
Hι	3771.715	3772.418	–0.628	0.209	RED	G400H
Hθ	3798.992	3798.887	0.181	–0.060	RED	G400H
Hη	3836.483	3836.959	–0.399	0.133	RED	G400H
Hζ	3890.169	3890.581	–0.334	0.111	RED	G400H
Ca II	3934.813	3934.964	–0.072	0.024	RED	G400H
Ca II	3969.571	3970.063	–0.413	0.138	RED	G400H
Fe I	4046.989	4047.398	–0.328	0.109	RED	G400H
Hδ	4102.928	4103.097	–0.087	0.029	RED	G400H
Fe I	4145.070	4145.185	–0.032	0.011	RED	G400H
Ca I	4227.956	4228.337	–0.296	0.099	RED	G400H
Fe I	4327.019	4327.103	0.003	–0.001	RED	G400H
Fe I	4384.818	4385.160	–0.254	0.085	RED	G400H
Hγ	4341.723	4342.224	–0.414	0.138	RED	G400H
Fe I	4406.028	4407.398	–1.282	0.428	RED	G400H
Hβ	4862.740	4863.467	–0.630	0.144	RED	G570H
Fe I	4921.929	4922.064	–0.036	0.008	RED	G570H
Fe I	4959.039	4960.360	–1.222	0.280	RED	G570H
Mg I	5168.813	5170.600	–1.684	0.386	RED	G570H
Mg I	5174.186	5174.970	–0.680	0.156	RED	G570H
Fe I	5329.583	5329.967	–0.277	0.064	RED	G570H
Na I	5891.667	5892.338	–0.553	0.127	RED	G570H
Na I	5897.636	5898.240	–0.486	0.111	RED	G570H
Hα	6564.696	6565.267	–0.440	0.101	RED	G570H

TABLE 3
Summary of Measured Internal/External Offsets

DET	DISP	$X_{internal} - X_{external}$ (diodes)	Dispersion (diodes)	# of Lines
BLUE	G130H	–0.186	0.070	5
BLUE	G190H	–0.073	0.087	8
BLUE	G160L	–0.084	0.101	10
BLUE	Mean	–0.102	0.100	23
RED	G190H	+0.174	0.145	16
RED	G270H	+0.200	0.073	51
RED	G400H	+0.104	0.113	14
RED	G570H	+0.153	0.108	9
RED	Mean	+0.176	0.105	90

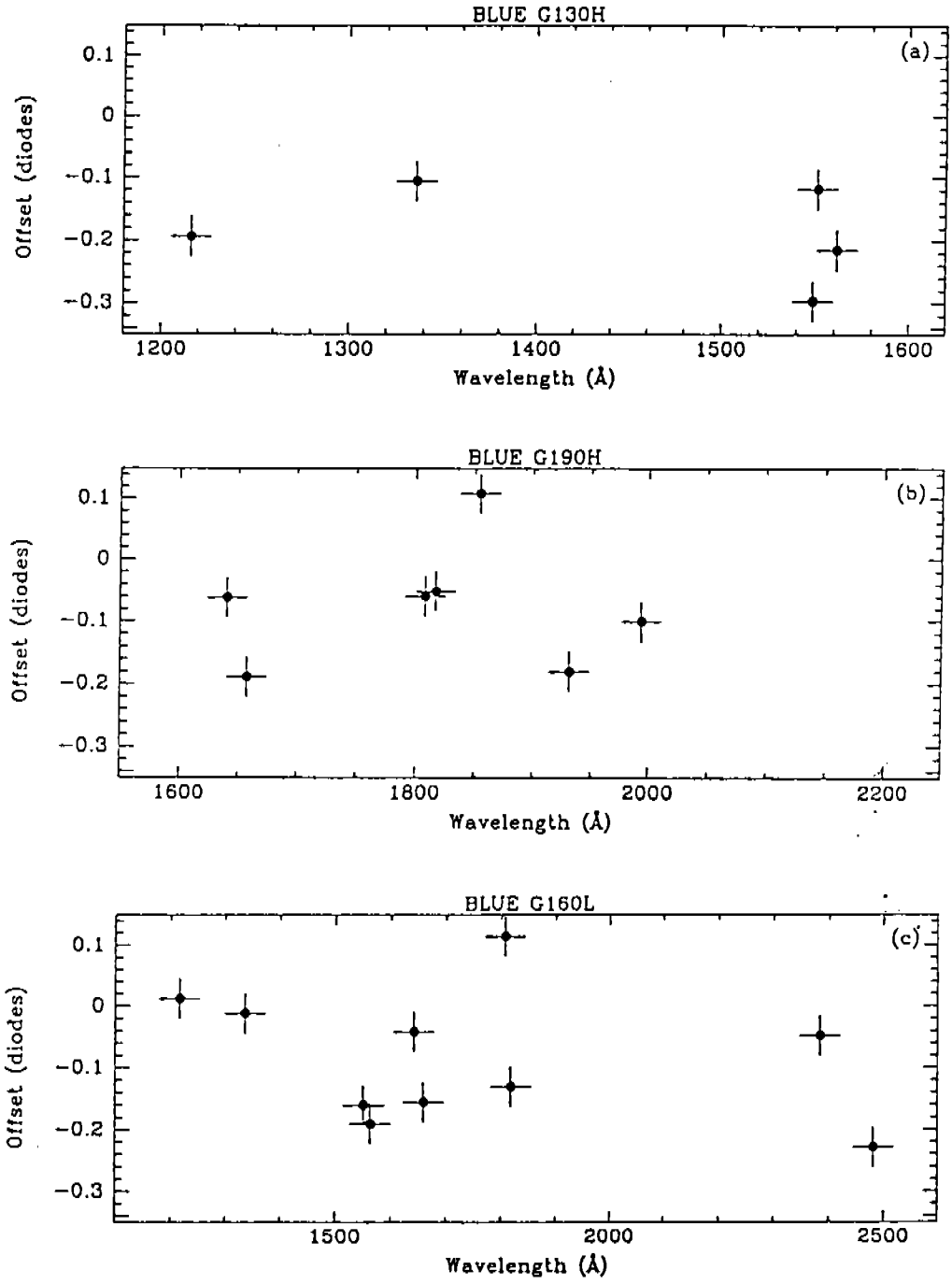

Figure 1 — Panels (a) through (g) show the observed offsets ($X_{internal} - X_{external}$) in diodes versus wavelength for each grating. The vertical height of the crosses on each point is the typical 1σ error in measurement for a line centroid (~0.05 diode). Fainter lines have larger errors, but no larger than 0.15 diode; brighter lines have smaller errors.

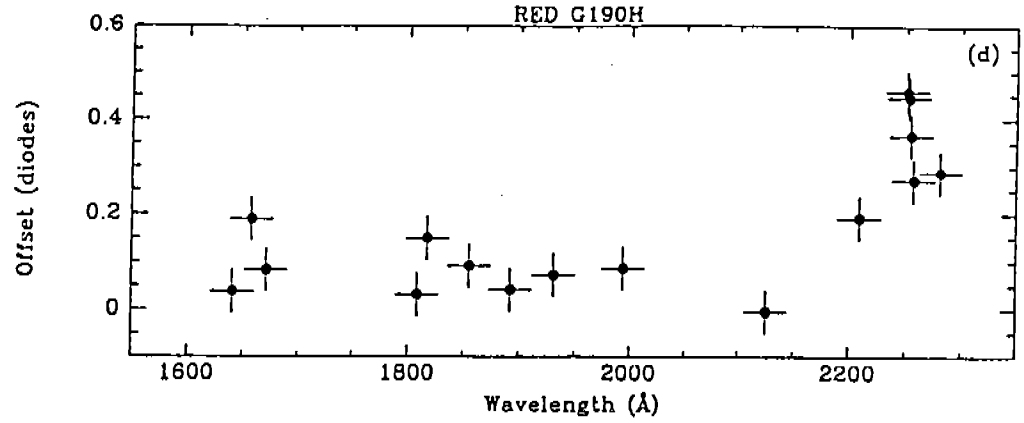
RED G190H
(d)
Offset (diodes)
0.6
0.4
0.2
0
1600
1800
2000
2200
Wavelength (Å)

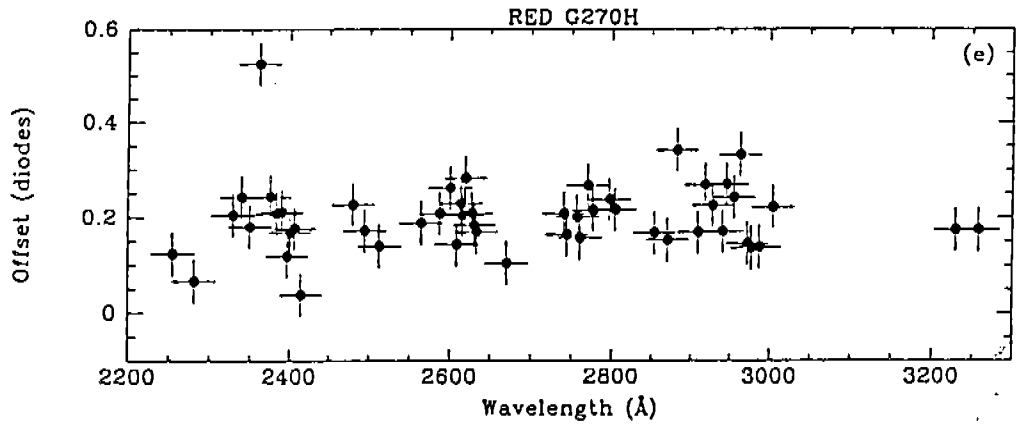
RED G270H
(e)
Offset (diodes)
0.6
0.4
0.2
0
2200
2400
2600
2800
3000
3200
Wavelength (Å)

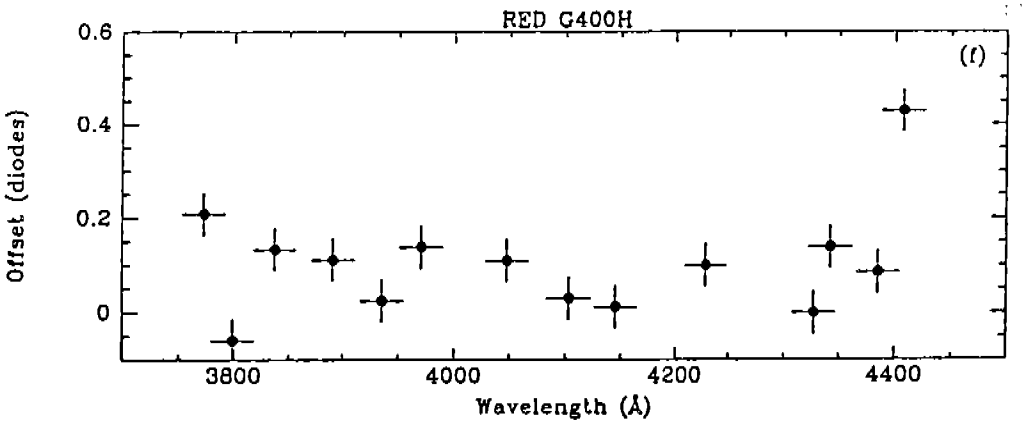
RED G400H
(f)
Offset (diodes)
0.6
0.4
0.2
0
3800
4000
4200
4400
Wavelength (Å)

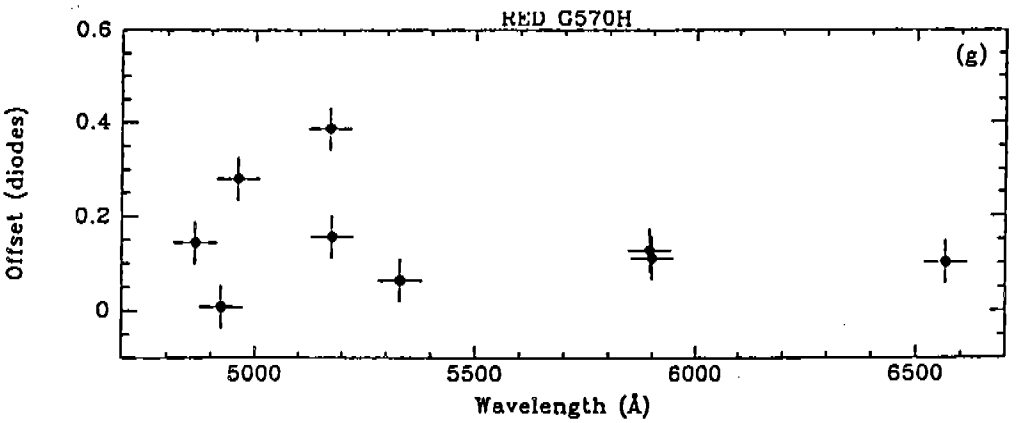
RED G570H
(g)
Offset (diodes)
0.6
0.4
0.2
0
5000
5500
6000
6500
Wavelength (Å)